Modeling Three-Terminal III-V/Si Tandem Solar Cells

Preprint

Emily L. Warren, Michael G. Deceglie, Paul Stradins, and Adele C. Tamboli
National Renewable Energy Laboratory

Presented at 2017 IEEE 44th Photovoltaic Specialists Conference (PVSC)
Washington, DC
June 25–30, 2017

NREL is a national laboratory of the U.S. Department of Energy
Office of Energy Efficiency & Renewable Energy
Operated by the Alliance for Sustainable Energy, LLC

This report is available at no cost from the National Renewable Energy Laboratory (NREL) at www.nrel.gov/publications.

Conference Paper
NREL/CP-5J00-67774
June 2017

Contract No. DE-AC36-08GO28308

NOTICE

This report is available at no cost from the National Renewable Energy Laboratory (NREL) at www.nrel.gov/publications.

Available electronically at SciTech Connect http:/www.osti.gov/scitech

Available for a processing fee to U.S. Department of Energy and its contractors, in paper, from:

U.S. Department of Energy
Office of Scientific and Technical Information
P.O. Box 62
Oak Ridge, TN 37831-0062
OSTI http://www.osti.gov
Phone: 865.576.8401
Fax: 865.576.5728
Email: reports@osti.gov

Available for sale to the public, in paper, from:

U.S. Department of Commerce
National Technical Information Service
5301 Shawnee Road
Alexandria, VA 22312
NTIS http://www.ntis.gov
Phone: 800.553.6847 or 703.605.6000
Fax: 703.605.6900
Email: orders@ntis.gov

Cover Photos by Dennis Schroeder: (left to right) NREL 26173, NREL 18302, NREL 19758, NREL 29642, NREL 19795.

NREL prints on paper that contains recycled content.

Modeling three-terminal III-V/Si tandem solar cells

Emily L. Warren, Michael G. Deceglie, Paul Stradins, Adele C. Tamboli

National Renewable Energy Laboratory, 15013 Denver West Parkway, Golden, CO 80401, USA

***Abstract* — Three-terminal (3T) tandem cells fabricated by combining an interdigitated back contact (IBC) Si device with a wider bandgap top cell have the potential to provide a robust operating mechanism to efficiently capture the solar spectrum without the need to current match sub-cells or fabricate complicated metal interconnects between cells. Here we develop a two dimensional device physics model to study the behavior of IBC Si solar cells operated in a 3T configuration. We investigate how different cell designs impact device performance and discuss the analysis protocol used to understand and optimize power produced from a single junction, 3T device.**

***Index Terms* — tandem solar cell, three-terminal, Sentaurus, TCAD, modeling**

I. Introduction

There has been a great deal of recent interest in the development of III-V/Si tandem solar cells, with multiple new efficiency records set in the past year [1], [2]. Most tandem solar cells designs are either two-terminal (2T) devices, where the subcells are electrically connected in series, or 4 terminal (4T) devices, where each subcell is operated independently. While 2T devices are more common, recent modeling has shown that 4T devices are more resilient to variations in solar spectrum and can produce higher energy yield [3], [4]. An alternative cell configuration that has potential to combine the strengths of both is a three-terminal (3T) device consisting of a III-V top cell optically in series with an interdigitated back contact (IBC) Si cell. Such a 3T tandem can be run either in a standard 2T configuration, or use the second back contact to extract excess current, making the device less sensitive to current matching between the subcells due to bandgap differences or spectral varation. If all of the excess photocurrent can be extracted from the Si bottom cell in a GaInP/Si tandem, the overall efficiency of the device would increase by $\sim$5% absolute above the performance of a 2T tandem.

A 3T contacting geometry has the potential to benefit multiple approaches to creating tandem cells. These cells would not need lateral current extraction between the cells (which is required for 4T operation), enabling the use of transparent conductive adhesives (TCAs) or other low cost conductive layers [5]. However, there are unique design features of the 3T geometry that may detrimentally impact performance (such as the need for a conductive top surface in an IBC Si cell) that motivates the detailed modeling of this relatively unexplored tandem cell design.

The modeling of most tandem cells in the literature has been carried out by combining 1D solar cell models (e.g. PC1D) with separate circuit models or simply adding together the performance of the two subcells. While this is sufficient to capture the behavior of a 2T or 4T device, to accurately model the behavior of a 3T cell as described above requires at least a 2D model that is capable of handling device physics in two dimensions and with more than 2 contacts. There are no dedicated solar cell modeling software packages that meet this requirement, necessitating the use of a more powerful simulation environment. In this work, we have used a technology computer aided design (TCAD) software package to understand the performance of a 3T solar cell based on an IBC Si bottom cell.

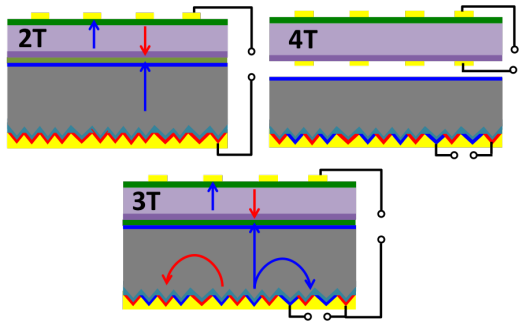

Fig. 1. Schematic comparing 2T, 3T, and 4T cell configuration. 2T devices are limited by current matching conditions, but offer simpler integration than 4T devices. 3T devices can leverage advantages of both approaches.

II. Simulation Methods and Parameters

The electrical simulations presented here were performed using Sentaurus TCAD (Synopsis). The two-dimensional nature of an IBC cell structure requires a 2D structure with a width equal to the pitch between the*p* and*n* type back contacts. The cell geometry was roughly based on the polysilicon on oxide (POLO) IBC cell developed at the Institute for Solar Energy Research Hamelin (ISFH), although the device structure was not optimized to fully match experimental data [6].

A. Optical Generation

Due to the vastly different length scales needed to capture the electrical and optical performance of an IBC device, the optical generation profile was calculated separately and then used to solve the device physics of the cell [7]. This enables the optical generation profile to guide the meshing of the device area, so that regions of high optical absorption are meshed more densely, which enhances the efficiency of convergence of the device physics model. Optical generation profiles were created within Sentaurus or using PV Lighthouse's module ray-tracing software [8]. All of the results presented here were calculated using the AM1.5G spectrum without any filtering from a top III-V cell or TCA layer. The optical stack included a standard 75 nm antireflective coating layer so that the simulated performance under standard illumination conditions

TABLE I
GEOMETRY OF SI CELL

Parameter	Value
Cell thickness	160 μm
Unit cell width	365 μm
poly-Si thickness	20 nm
Front contact parameters	
Tunnel oxide thickness	1.5 nm
P In-diffusion depth	300 nm
P In-diffusion peak	10^{19} cm^{-3}

TABLE II
DEVICE PARAMETERS FOR SI CELL

Parameter	Value
Temperature	300 K
Bulk doping	(P) 10^{15} cm^{-3}
Bulk lifetime	2 ms
SRV at Si/SiO_2 interface	10^3 cm/s
SRV at Si/SiN_x interface	50 cm/s
SRV at metal contacts	10^7 cm/s
Tunneling model	Nonlocal tunneling
Tunneling effective mass ($m_{e,h}$)	0.4

can be more directly compared to standard single junction Si solar cells.

B. Electrical Simulation

The geometry of the device is shown in figure 2a and consists of an *n*-type Si substrate with back contacts defined by poly-Si *p* and *n* regions that are then contacted with smaller area metal openings that are contacted with Al. The entire front surface of the cell was coated with n-poly Si and then contacted with a transparent uniform contact to simulate a TCA layer. The basic geometric parameters of the cell are listed in Table I. For simplicity, the poly-Si layers are defined as separate c-Si regions with different doping densities [9], [10]. Gaussian doping profiles were used to simulating in-diffusion of dopants into the bulk. Different front surface conditions were investigated to understand the impact of passivation and recombination on 3T performance. A passivated front contact was modeled with a carrier selective contact using a thin tunneling SiO_2 layer, as has been previously demonstrated [10], [11]. An ohmic front contact (SRV = 10^7 cm/s) was modeled to provide an upper bound for the degradation of cell performance due to recombination at the front surface. The basic material parameters used to define the properties of the materials used are listed in Table II.

The device physics of the cell was solved using Sentaurus Device. To improve convergence of the model, the illumination was slowly turned on over multiple steps and then a quasi-stationary ramp was used to sweep the voltage of the *p* contact from 0V to 0.8V to extract the current voltage behavior of the cell. For 3T operation, another quasi-stationary ramp was used to set the current from one of the two*n* contacts prior to sweeping the voltage of the *back-p* contacts.

III. RESULTS AND DISCUSSION

For our proposed 3T tandem cell to work it must be possible to extract the excess current from an IBC Si cell that is operating in series with a wider bandgap top cell with minimal losses to the overall performance of the device. We first examine each of the limiting 2T operating conditions for the simulated 3T Si cell.

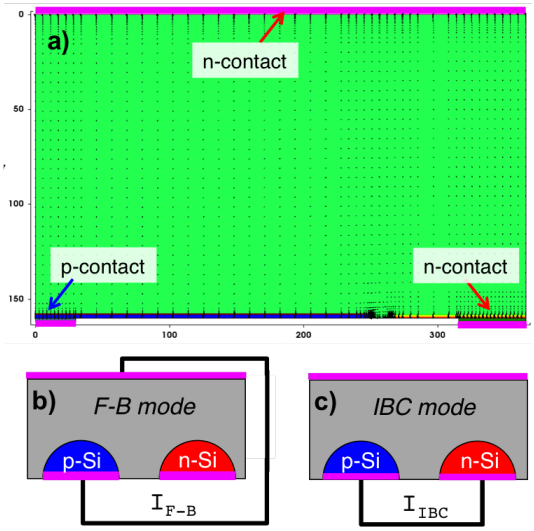

Fig. 2. a) TCAD model of a 3-terminal n-type Si cell with a n-type top contact and standard*n* and*p* IBC back contacts; simplified schematics of the two limiting operating modes of such a 3T cell: b) current extracted between *top-n* and *back-p* contact; c) current extracted between *back-n* contact and *back-p* contact.

There are two ways to extract power out a 3T Si cell, as shown in Fig 2. In the case of a cell with an n-type base, current can either be extracted between the front n-type contact of the cell and the back p-type contact (*F-B* mode, Fig 2b), or between the back n-type contact and the back p-type contact (*IBC* mode, Fig 2c).

We first investigate the limiting cases of performance for the device in the limiting 2T modes (*F-B* and *IBC*) under AM1.5G illumination to compare performance to standard 2T Si devices. It is well-documented that passivation of the front surface is critical to achieve high efficiencies for standard IBC cells, so it is important to determine whether a 3T device will suffer by having a conductive front surface. Figure 3 shows J-V data for cells operating in each mode with and without a passivating front contact (Figure of merit data for each device is compiled in Table III.) When the poly-Si/SiO_2 passivated front contact structure is replaced with an ohmic contact (SRV = 10^7 cm/s), the performance of the cell drops dramatically, from $>$22% to $<$17% absolute, in both *IBC* mode and *F-B* mode. This demonstrates the importance of a well-passivated surface for the operation of a device with a large area contact. Interestingly, in both cases the cell performs slightly better in *F-B* mode than in *IBC* cell, for otherwise identical cell geometries. The difference in performance can be attributed to improved fill-factor (FF). It has previously been suggested that the direct current path between the *back-p* and full area *front-n* contact can minimize current bunching at localized contacts and improve FF, which also seems to improve performance in this simulation [10].

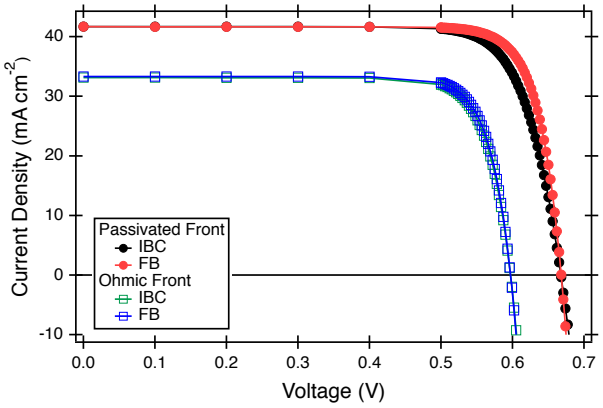

Fig. 3. J-V plots for a 3T Si cell, operated in either *IBC* mode (black) or *F-B* mode (red). Solid markers are for a device with a passivated front contact, open squares for an ohmic front contact.

Debate exists in the literature over the mechanism of passivation for poly-Si/ SiO_2/Si junctions [10], [12], so we compare the tunneling model to an idealized c-Si/poly-Si interface where the SRV is set to a value of 10 cm/s to represent an idealized passivated contact. The performance of these cells is very similar to those with an active tunneling layer, but the open circuit voltages (V_{oc}) of these devices were lower than when tunneling was activated. This suggests that the tunneling mechanism may play a role in the high V_{oc}s reported for experimental passivated contact cells.

In 3T mode, the cell's operating range has an extra degree of freedom, requiring two independent variables to specify the operating point of the cell. Since each n-type contact can create a different diode with the common p-type contact, each sub-circuit can sustain a different voltage. It is important to account for the power generated in each sub-circuit, not just the current-voltage behavior at any given operating condition of the cell. When the current at either n-type contact was set to a constant value (as might be the case for a tandem cell with the top cell connected in series to one sub-circuit), the total power out of both circuits matches or exceeds the 2T performance in *IBC* or *F-B* mode.

IV. Conclusion

We have developed a 2D TCAD model to investigate the performance of 3T Si IBC cells for integration into a 3T tandem cell. Operating a tandem cell in such a configuration enables much simpler fabrication techniques than a 4T geometry, as no lateral conduction is needed between the top and bottom cells to extract current. It still enables more efficient utilization of all the available photocurrent than in a 2T configuration, where the total current is always limited by one of the subcells. We show that 3T cell designs utilizing a passivated front and two IBC back contacts enables Si devices to be operated in multiple modes with similar overall power conversion. This provides a pathway to new routes to high efficiency 3T Si-based tandem solar cells.

TABLE III
FIGURES OF MERIT FOR OPERATION OF 3T SI CELL IN IBC AND F-B MODE UNDER DIFFERENT FRONT CONTACT CONDITIONS

Configuration	Voc (mV)	Jsc (mA cm^{-2})	FF	Eff (%)
IBC, passivated front	668	41.69	79.1	22.0
F-B, passivated front	668	41.69	82.2	22.9
IBC, ohmic front	597	33.14	81.2	16.1
F-B, ohmic front	597	33.32	81.7	16.3
IBC, no tunnel oxide	661	41.56	82.5	22.6
F-B, no tunnel oxide	662	41.56	82.7	22.7

Acknowledgment

The authors thank Michael Rienacker (ISFH), Manuel Schnabel, Henning Schulte-Huxel, Robby Peibst (ISFH), and Ana Kavence for helpful discussions. Funding for this work at NREL was provided by DOE through EERE contract SETP DE-EE00030299 and under Contract No. DE- AC36-08GO28308. The United States Government retains and the publisher, by accepting the article for publication, acknowledges that the United States Government retains a non-exclusive, paid-up, irrevocable, world- wide license to publish or reproduce the published form of this manuscript, or allow others to do so, for United States Government purposes.

References

[1] S. Essig, M. A. Steiner, C. Allebe, J. F. Geisz, B. Paviet-Salomon, A. Descoeudres, V. LaSalvia, L. Barraud, N. Badel, A. Faes, J. Levrat, M. Despeisse, C. Ballif, P. Stradins, and D. L. Young, "Realization of GaInP/Si Dual-Junction Solar Cells With 29.8% 1-Sun Efficiency," *J. of Photovoltaics*, vol. 6, no. 4, pp. 1012–1019, 2016.

[2] R. Cariou, J. Benick, P. Beutel, N. Razek, C. Fl, M. Hermle, D. Lackner, S. W. Glunz, S. Member, A. W. Bett, M. Wimplinger, and F. Dimroth, "Monolithic Two-Terminal III – V // Si Triple-Junction Solar Cells with 30.2% Efficiency under 1-Sun AM1.5G," *J. of Photovoltaics*, vol. 7, no. 1, pp. 367–373, 2017.

[3] H. Liu, Z. Ren, Z. Liu, A. G. Aberle, T. Buonassisi, and I. M. Peters, "The realistic energy yield potential of GaAs-on-Si tandem solar cells: a theoretical case study," *Optics Express*, vol. 23, no. 7, p. A382, 2015.

[4] S. Essig, S. Ward, M. A. Steiner, D. J. Friedman, J. F. Geisz, P. Stradins, and D. L. Young, "Progress Towards a 30% Efficient GaInP/Si Tandem Solar Cell," *Energy Procedia*, vol. 77, pp. 464–469, 2015.

[5] T. Klein, B. Lee, M. Schnabel, E. Warren, P. Stradins, A. Tamboli, and M. van Hest, "Transparent conductive adhesives for tandem solar cells," *Proceedings of the 44th IEEE PVSC*, 2016.

[6] F. Haase, F. Kiefer, S. Schäfer, C. Kruse, J. Krügener, R. Brendel, and R. Peibst, "Ibc solar cells with polycrystalline on oxide (polo) passivating contacts for both polarities," *Japanese Journal of Applied Physics*, 2017.

[7] "Optimization of Rear Contact Design in Monocrystalline Silicon Solar-Cell Using 3D TCAD Simulations," Synopsis, Tech. Rep., 2011.

[8] (2017, June) PV Lighthouse: Module Ray Tracer. [Online]. Available: https://www.pvlighthouse.com.au

[9] U. Römer, R. Peibst, T. Ohrdes, B. Lim, J. Krügener, E. Bugiel, T. Wietler, and R. Brendel, "Solar Energy Materials & Solar Cells Recombination behavior and contact resistance of n and p poly-crystalline Si / mono-crystalline Si junctions," *Solar Energy Materials and Solar Cells*, vol. 131, pp. 85–91, 2014.

[10] H. Steinkemper, F. Feldmann, M. Bivour, and M. Hermle, "Numerical Simulation of Carrier-Selective Electron Contacts Featuring Tunnel Oxides," *IEEE Journal of Photovoltaics*, vol. 5, no. 5, pp. 1348–1356, 2015.

[11] H. Steinkemper, F. Feldmann, M. Bivour, and M. Hermle, "Theoretical Investigation of Carrier-selective Contacts Featuring Tunnel Oxides by Means of Numerical Device Simulation," *Energy Procedia*, vol. 77, no. 5, pp. 195–201, 2015.

[12] R. Brendel and R. Peibst, "Contact Selectivity and Efficiency in Crystalline Silicon Photovoltaics," *J. of Photovoltaics*, vol. 6, no. 6, pp. 1413–1420, 2016.